

Formation of Chain-Folded Structures in Supercooled Polymer Melts

Hendrik Meyer^{1,2} and Florian Müller-Plathe²

¹*Institut Charles Sadron, C.N.R.S., 6, rue Boussingault, 67083 Strasbourg, France*

²*Max-Planck-Institut für Polymerforschung, 55021 Mainz, Germany*

(June 21, 2021)

The formation of chain-folded structures from the melt is observed in molecular dynamics simulations resembling the lamellae of polymer crystals. Crystallization and subsequent melting temperatures are related linearly to the inverse lamellar thickness. Analysis of the single chain conformations in the crystal shows that most chains reenter the same lamella by tight backfolds. Simulations are performed with a mesoscopic bead-spring model including a specific angle bending potential. They demonstrate that chain stiffness alone, without an attractive inter-particle potential, is a sufficient driving force for the formation of chain-folded lamellae.

For polymeric materials, the connectivity of the long-chain molecules usually hinders the formation of perfect crystals. Instead, most crystallization conditions lead to partially crystalline structures consisting of a stacking of chain-folded lamellae and amorphous regions. There is nowadays wide agreement on the structure of this semicrystalline phase [1]. However, the pathway which leads to it and why it is taken is one of the unsettled questions in polymer science. Actively debated ideas [2–7] are intermediate mesomorphic phases [2] and the possibility of a spinodal mode [6–9] in contrast to nucleation and growth. Existing theories of polymer crystallization [10–12] are still considered incomplete [2, 5, 13, 14]. Thus, it is desirable to develop new tools for examining nucleation and crystal growth, and especially its early stage.

Computer simulations generally have two advantages which may help to understand the nonequilibrium process of polymer crystallization. First, the trajectories of all particles are available. This can give information about single molecules which are not accessible by experiments. Second, models of variable complexity can be simulated. The use of successive levels of approximations has the advantage to give insight into the effect of certain interactions separated from others. In this spirit, this Letter explains how chain-folded structures emerge from the supercooled melt when only the excluded volume and the possible conformations of the polymer chains are taken into account.

Many other simulation approaches have already been proposed in the context of polymer crystallization. Monte Carlo (MC) techniques were used to test theories of the lamellar thickness with lattice models [11, 15, 16]. On a larger length scale, MC was successfully applied

to model 2D crystallization [17]. Molecular dynamics (MD) is often more realistic, but simulations have been restricted either to few chains and short times [18], or to structure formation of very short chains [19–21], or to an isolated long chain which collapses into a “crystalline” globule [9, 22]. Recent MD simulation studies which come closest to our work deal with the crystallization of 20mers from the melt [19], of 10mers in thin films [21], and of few long chains from solution [23]. Here, we present large scale MD simulations of structure formation from the melt for a wide range of chain lengths and temperatures. We examine the homogeneous nucleation regime, since no walls or starting nuclei are introduced. In this Letter, we demonstrate in particular that systems of chains long enough to fold can be simulated from the amorphous melt up to the chain-folded lamella. The individual particle trajectories are then used to analyze the nucleation process and the chain folding in detail.

We use a simplified version of a model for poly(vinyl alcohol) (PVA) derived by a systematic coarse-graining procedure [24] from fully atomistic simulations. A coarse-grained bead represents one monomeric unit of PVA. (In contrast, the often used united-atom models [19, 20, 23] consider one bead per carbon.) The beads are connected by harmonic springs, and additionally interact by an angle bending potential retaining information on the torsional states of the atomistic backbone. The nonbonded interactions are approximated by a Lennard-Jones 6-9 potential. Furthermore, for the simulation of a dense melt, it is sufficient to take only the repulsive part of the potential [25]. This leads to some shift of energy and pressure while it affects only little the qualitative behavior of the system. This approximation speeds up the simulation. But it also switches off one possible driving force of crystallization, the cohesive energy, which would increase with decreasing temperature. Thus, when lowering temperature, only the chain stiffness will increase.

Our model is defined by several parameters [26]. Length scales are fixed by the mapping from atomistic simulations. Units are reported in $\sigma = 0.52$ nm corresponding roughly to the chain diameter of PVA. The bond length is $0.5\sigma = 0.26$ nm. In these units, the density is about 2.1 monomers per σ^3 . The nonbonded potential between monomers is $V(r)/k_B = -0.75/r^6 + 0.53/r^9$ which is cut and shifted to zero at the minimum $r_{\text{cut}} = 1.02\sigma$. Nonbonded interactions between first and second neighbors along each chain are excluded. The angle potential shown in Fig. 1 has three minima at 180° , 126° ,

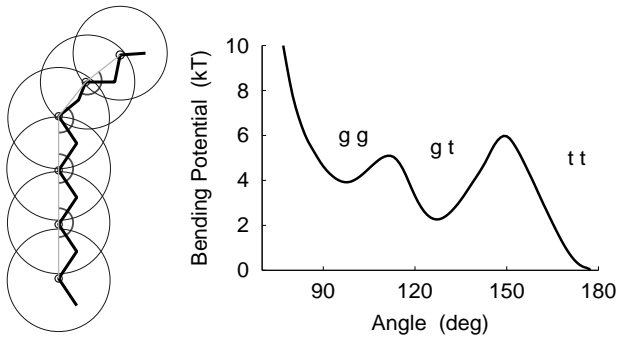


FIG. 1. Sketch of the coarse-grained model “CG-PVA”. Each bead represents a monomer with two carbon atoms on the backbone. Successive beads are connected by harmonic springs. Three successive beads interact via the shown angle bending potential.

and 95° corresponding to trans–trans, trans–gauche, and gauche–gauche conformations of the atomistic backbone chain. Note that this model, though initially fitted to represent PVA, is also suitable for polyethylene which has almost the same dimensions as PVA. The equations of motion are integrated by the velocity-Verlet algorithm using a timestep of 0.005τ [27]. Temperature is kept constant through a Langevin-thermostat with friction constant $\Gamma = 0.5$. Temperatures and energies are expressed in dimensionless units with $m = k_B = 1$; $T = 1$ corresponds to the high temperature phase of the amorphous melt. Constant pressure is imposed by the isotropic Berendsen manostat [28]. The simulations are performed in a cubic box with periodic boundary conditions.

The model is studied for chain lengths $N = 10, 20, 50,$ and 100 by two kinds of experiments. The first consists in cooling at constant rate, the second is isothermal relaxation: the system is suddenly quenched to a temperature T_c below the melting temperature. In both cases we start with an amorphous configuration equilibrated at $T = 1$. Figure 2 shows the volume as a function of temperature in cooling and heating cycles. It decreases with temperature; a sudden drop of the volume is attributed to a phase transformation. Note the hysteresis. Indeed, crystallization only takes place when a stable nucleus is formed, i.e. at a certain supercooling below the melting temperature. In addition, the hysteresis is enlarged due to the fast cooling and heating rates. Once formed, a crystal is also stabilized by the periodic boundary conditions which lead to a higher melting temperature.

Figure 2 also shows that shorter chains begin to crystallize at lower temperatures than longer chains. Similarly, the decamers melt at lower T_m than the icosamers. However, still longer chains melt at about the same temperature as the icosamers. Furthermore, the volume change for $N = 50$ and $N = 100$ is less pronounced than for $N = 20$. Both observations indicate that the crystallinity of these samples is far from 100%. In fact, the shorter chains $N = 10$ and $N = 20$ always form ex-

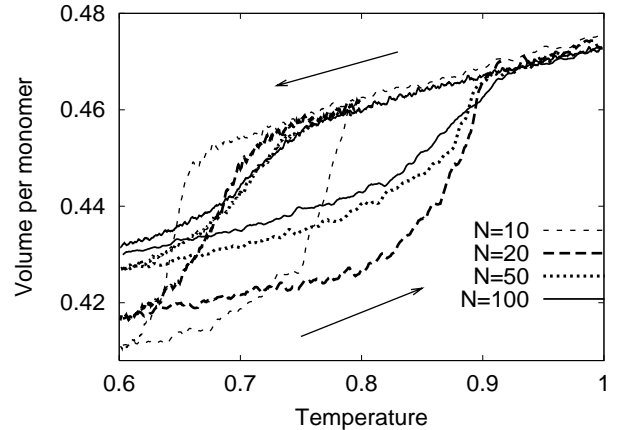


FIG. 2. Volume dependence in cooling/heating cycles for different chain lengths. The cooling rate is $5 \times 10^{-6} \tau^{-1}$, the heating rate $2 \times 10^{-5} \tau^{-1}$.

tended chain crystals. At temperatures below $T \approx 0.7$, crystallization sets in immediately and small domains are formed similar to those reported in Ref. [19]. For smaller temperature jumps, the formation of a single nucleus is observed which grows in regular layers. More details will be given elsewhere [26].

Let us focus on the longest chains, $N = 100$, in the following. They always form folded lamellar structures (see Fig. 3). The stems (the completely stretched parts) are much longer at higher temperature. Furthermore, the structure factor (not shown) indicates long range order with Bragg peaks of the hexagonal lattice. The structure factor also has a peak at small wave vectors corresponding to the thickness of the crystal lamella. In Ref. [26] we discuss an alternative way of determining the lamellar thickness with the bond orientation correlation function. It gives an upper bound of the stem length. Since most chains form tight backfolds (see below), this is a good estimate of the lamellar thickness. Figure 4 shows that the inverse of this average stem length increases linearly with decreasing T_c , a relation observed experimentally for most crystallizing polymers. The same holds for the melting temperature of the corresponding structures. At $T_c = 0.7$, most chains form 3 folds, at $T_c = 0.74$ they have mostly 2 folds. At $T_c = 0.78$ the first nucleus grows with once-folded chains; however, it continues to grow with a mixture of once and twice folded chains which do not unfold during the simulation time. At $T_c = 0.8$, finally, most chains exhibit only one fold.

This can be summarized as follows: the higher the temperature the better the crystal. Though perhaps paradoxical at first sight, this is generally observed for crystallizing systems and in particular for polymers because the thermodynamically favorable extended chain crystal is kinetically not accessible. For a single chain, crystallizing with many folds is much closer to the initial coil state in the melt than a once folded or even extended

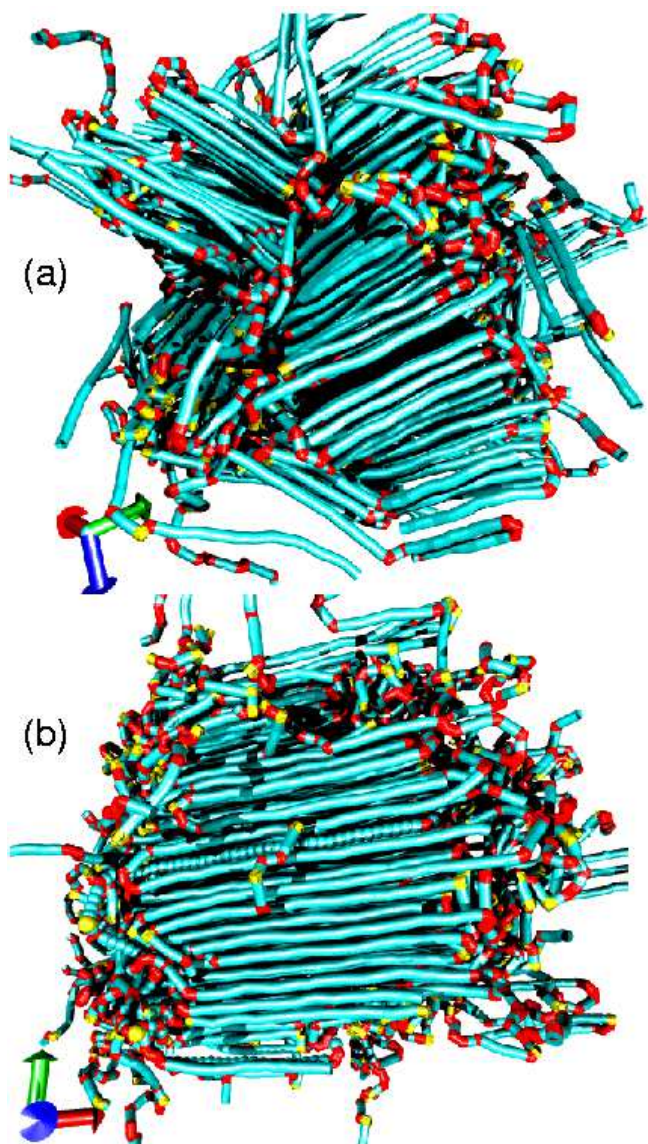


FIG. 3. (color) Two examples of structures obtained at temperatures $T_c = 0.7$ (a) and $T_c = 0.8$ (b) with 192 chains of $N = 100$ monomers. Note the larger lamellar thickness at $T_c = 0.8$. At $T_c = 0.7$, two smaller domains with different orientation are formed. Color coding is according to the bond angle (cf. Fig. 1): blue=tt, red=gt, yellow=gg. The box length is about 10 nm. Note that periodic boundary conditions are applied; chains are not cut but mapped with their center of mass into the central box.

chain. So, at lower temperatures, when the mobility is lower and the nucleation probability is higher, the chains will end up in crystals of short stems before having time to unfold. The barrier between crystals of different fold lengths is high and is overcome only with additional activation, for example, by annealing.

All simulation results reported so far are consistent with the interpretation of well known experimental findings. This gives us confidence in the model proposed. On this basis, we may use the simulation as a nanoscope

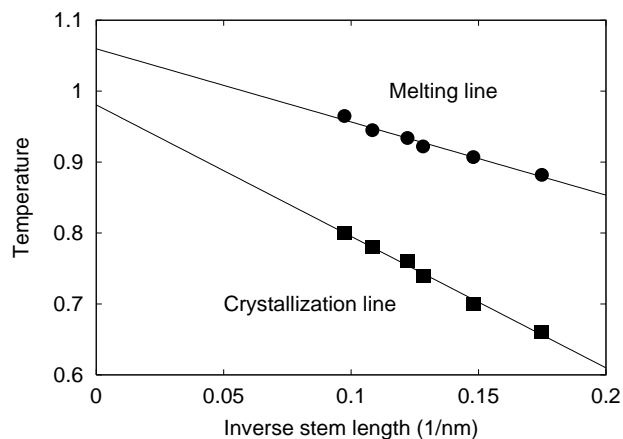


FIG. 4. Dependence of lamellar thickness on the crystallization temperature and melting temperature of the corresponding final structures. The lines are linear fits. Melting temperatures are rather overestimated due to finite size effects.

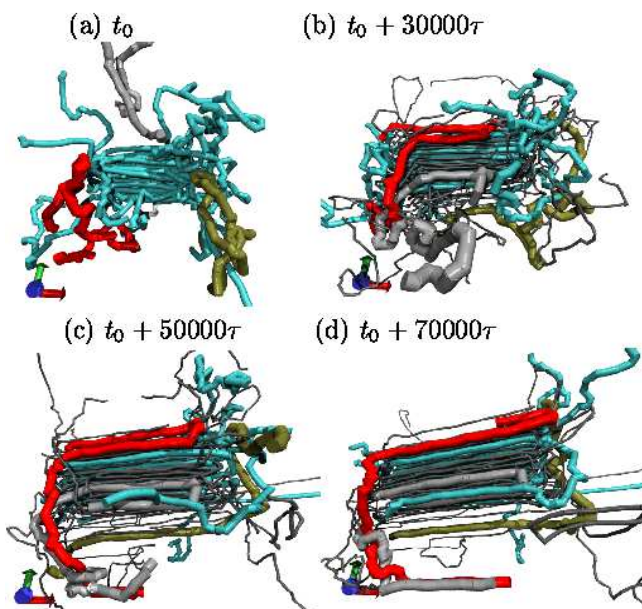


FIG. 5. (color) Snapshots of the crystallization at $T_c = 0.8$. (a) The 13 chains participating in the initial nucleus are shown (blue). The following snapshots contain 20 more chains (thin lines) which align to the crystal in the first 40000τ . (b) The red chain is partly attaching to the crystal front. (c) The hairpin of this chain is growing to fill the whole lamellar thickness. (d) Finally, the hairpin is vanishing: the chain glides until having only two stems in the crystal and a large bridge on the fold surface.

and visualize the evolution of single chains as well as the conformations of the chains in the crystal. Figure 5 illustrates snapshots from the crystallization at $T_c = 0.8$. In this case a slightly different temperature protocol was applied: the start nucleus was obtained by quenching the melt from $T = 1.0$ to $T = 0.7$ over 10000τ . Then, the temperature was raised to $T = 0.8$ which ultimately leads to the structure in Fig. 3b after 140000τ . Initially,

the nucleus grows primarily in the direction of the stems (a,b). Later on, further stems reorient and “attach” to the primary nucleus. This “attachment” can start with arbitrary parts of the chain. However, the chains move until aligning their ends with the existing crystal. In the sequence of Fig. 5 one chain is highlighted which joins the crystal in a complicated way. It attaches first via a hairpin which advances until aligning with the total stem length of the crystal (c). However, the other end of this chain is quite far. The chain slides along its contour to finally annihilate the hairpin.

A quantitative analysis of the single chain conformations results in 3/4 of the folds in the final structure at $T_c = 0.8$ being backfolds. One third of them are hairpin folds, only 1/4 of the backfolds reenter the crystal farther than at the 3rd neighbor position. At lower T_c , the fraction of backfolds in our samples was found to be around 60%. Due to domain formation (Fig. 3a), up to 25% of the folds link stems participating in different domains. The distribution of the re-entry distances of backfolds is almost the same for all crystallization temperatures.

In summary, this Letter highlights results of a versatile model suitable for studying the chain-folding process of polymer crystallization. The chosen level of coarse-graining retains enough information on the local conformations while the speed-up due to the reduction of details is sufficient to follow nucleation and growth from the melt up to chain-folded structures. Starting from the chemistry of PVA, the model finally consists only of excluded volume interaction and a specific angle bending potential favoring stretched conformations and allowing precise fold states; there is no explicit attraction between monomers. We understand the crystallization in our model as driven by an energetic and an entropic component. When lowering temperature, energy leads through the angle potential (Fig. 1) to an increased chain stiffness (the persistence length of an isolated, free chain passes from 3.4 monomers at $T = 1.0$ to 6 monomers at $T = 0.7$). Entropy favors the parallel ordering as in liquid crystal [29], because the gain in translational entropy of the ordered structure at lower temperature is possibly much larger than the loss in conformational entropy. The temperature dependent kinetics then determines the form of the nonequilibrium structures of chain-folded lamellae. Yet, the qualitative chain length dependence of crystallization and melting temperatures (Fig. 2) as well as the lamellar thickness behavior (Fig. 4) match well experimental findings. This underlines that the orientational and conformational ordering play a major role for polymer crystallization. It further suggests that crystallization might pass through an intermediate step of liquid crystalline order before locking in into the final crystal structure [7], at least in a region in front of the growth front. The model could now be used to address questions of recent crystallization experiments in confined geometries and, with larger systems, the open

question of a spinodal initiation of crystallization.

We thank K. Kremer, J. Baschnagel, B. Lotz, and J.-U. Sommer for fruitful discussions. HM acknowledges financial support by European Associated Laboratories MPI-P/ICS.

-
- [1] See e.g. P. J. Barham, in Vol. 12 of *Materials Science and Technology*, edited by Cahn, Haasen, and Kramer (VCH, Weinheim, 1992), Chap. 4.
 - [2] G. Strobl, *Eur. Phys. J. E* **3**, 165 (2000).
 - [3] B. Lotz, *Eur. Phys. J. E* **3**, 185 (2000).
 - [4] S. Z. D. Cheng, C. Y. Li, and L. Zhu, *Eur. Phys. J. E* **3**, 195 (2000).
 - [5] M. Muthukumar, *Eur. Phys. J. E* **3**, 199 (2000).
 - [6] A. J. Ryan *et al.*, *Faraday Discuss.* **112**, 13 (1999).
 - [7] P. D. Olmsted *et al.*, *Phys. Rev. Lett.* **81**, 373 (1998).
 - [8] M. Imai, K. Kaji, and T. Kanaya, *Phys. Rev. Lett.* **71**, 4162 (1993).
 - [9] M. Muthukumar and P. Welch, *Polymer* **41**, 8833 (2000).
 - [10] J. D. Hoffman and R. L. Miller, *Polymer* **38**, 3151 (1997).
 - [11] D. M. Sadler and G. H. Gilmer, *Phys. Rev. Lett.* **56**, 2708 (1986).
 - [12] K. A. Armistead and G. Goldbeck-Wood, *Adv. Polym. Sci.* **100**, 221 (1992).
 - [13] J.-J. Point and J. J. Janimak, *Polymer* **26**, 7123 (1997).
 - [14] P. H. Geil, *Polymer* **41**, 8983 (2000).
 - [15] J. P. K. Doye and D. Frenkel, *Phys. Rev. Lett.* **81**, 2160 (1998). J. P. K. Doye, *Polymer* **41**, 8857 (2000).
 - [16] K. L. Anderson and G. Goldbeck-Wood, *Polymer* **41**, 8849 (2000).
 - [17] G. Reiter and J.-U. Sommer, *Phys. Rev. Lett.* **80**, 3771 (1998). J.-U. Sommer and G. Reiter, *J. Chem. Phys.* **112**, 4384 (2000).
 - [18] B. Sumpter, D. W. Noid, G. L. Liang, and B. Wunderlich, *Adv. Polym. Sci.* **116**, 73 (1994).
 - [19] H. Takeuchi, *J. Chem. Phys.* **109**, 5614 (1998).
 - [20] S. Fujiwara and T. Sato, *Phys. Rev. Lett.* **80**, 991 (1998).
 - [21] T. Shimizu and T. Yamamoto, *J. Chem. Phys.* **113**, 3351 (2000).
 - [22] Q. Liao and X. Jin, *J. Chem. Phys.* **110**, 8835 (1999).
 - [23] C. Liu and M. Muthukumar, *J. Chem. Phys.* **109**, 2536 (1998).
 - [24] D. Reith, H. Meyer, and F. Müller-Plathe, *cond-mat/0008338*, accepted by *Macromolecules*.
 - [25] K. Kremer and G. S. Grest, *J. Chem. Phys.* **92**, 5057 (1990).
 - [26] H. Meyer and F. Müller-Plathe, in preparation (2000).
 - [27] M. Allen and D. Tildesley, *Computer Simulation of Liquids* (Oxford Science, Oxford, 1987).
 - [28] H. J. C. Berendsen *et al.*, *J. Chem. Phys.* **81**, 3684 (1984).
 - [29] Note that our model chain is still flexible and has no intrinsically stiff parts as liquid crystalline polymers.